2019 IEEE International Ultrasonics Symposium (IUS)
Glasgow, Scotland, October 6-9, 2019

A General Framework for Channel Domain SVD Clutter Filtering

Kathryn Ozgun and Brett Byram

***Abstract*—Eigen-based clutter filtering of Doppler data has demonstrated greater clutter rejection performance than traditional filtering in a number of studies. However, practical translation of these eigen-based techniques to channel domain filtering applications is limited by their high computational burden. To enable efficient eigen-based filtering of channel data, we propose a domain-adaptive filtering framework. This technique involves using a basis set generated from RF data to filter delayed channel data. Preliminary findings suggest that this technique retains superior clutter rejection performance in comparison to conventional techniques.**

***Index Terms*—eigenvalue decomposition, singular value decomposition, power Doppler, clutter filter, channel data**

I. Introduction

Linear signal decomposition is a core component of clutter rejection. In the context of Doppler imaging, the objective of linear signal decomposition is to express a signal as a weighted sum of orthogonal basis functions, whereby blood and clutter signals may be separated. Clutter rejection is necessary for reliable visualization of blood flow, as clutter signals bias measures of velocity and power [1], [2], and can exceed the magnitude of weak blood echoes by 40-100 dB [3].

The efficacy of clutter rejection filters is predicated on the choice of basis set used to isolate a signal of interest. Basis sets are broadly defined via fixed or adaptive methods [4]. Fixed basis sets are composed of universal approximation functions, such as wavelets or complex modes of the Fourier series. In comparison, singular value decomposition (SVD) and eigenvalue decomposition (ED) techniques adaptively define basis functions using variance characteristics of the data.

Accordingly, traditional FIR and IIR filters which operate in the Fourier domain are effective when blood and clutter data reside in separable Fourier subspaces, *i.e.* exhibit unique frequency characteristics. However, the assumption of separable frequency characteristics is often violated; the frequency response of non-stationary tissue and acoustic clutter often overlaps low velocity blood echoes [5], [6], and electronic noise is considered a white noise process. This imposes a filter design trade-off between non-stationary clutter rejection and preservation of low velocity blood echoes.

Eigen-based (SVD and ED) filters have emerged as a robust alternative to traditional filters. Since the bases of eigen-based filters are defined by characteristics of the specific dataset, eigen-based filtering is inherently an adaptive technique. As a result, numerous studies have demonstrated that eigen-based filtering techniques may enable more robust rejection of clutter signal than traditional highpass filters [7].

Despite a substantial amount of literature on design considerations for eigen-based filtering [7], eigen-based filtering applications have been widely limited to beamformed IQ or RF data. Concurrently, several adaptive beamforming techniques have been developed for Doppler flow applications [8]–[12]. These beamformers rely on clutter rejection operations applied to channel data [10]–[12] or subaperture data [8], [9], respectively. In these contexts, the increased dimensionality of the data makes eigen-based filtering exceedingly computationally expensive.

We aim to reduce this computational burden by using a domain-adaptive methodology, in which a linear basis set derived from RF data is used to filter delayed channel data. This technique enables adaptive, eigen-based filtering schemes for large channel datasets, while maintaining reasonable computational cost. Preliminary efficacy is demonstrated using perfusion phantom data.

II. Conventional Eigen-Based Filtering

The proposed technique employs the general eigenvalue decomposition framework of [7], [13], [14] and lower-order singular value thresholding techniques of [7], [15], which we will briefly describe herein. An RF dataset is conventionally represented as a three dimensional matrix, with two dimensions corresponding to axial and lateral space (n_z and n_x) and one dimension in time (n_t). This data can be reshaped to combine the lateral and axial spatial extents, forming a Casorati matrix, $\mathbf{Y}$, with dimensions ($n_x n_z \times n_t$).

Eigenvalue decomposition is performed on the slowtime covariance matrix of $\mathbf{Y}$, yielding

$$\mathbf{Y}^{*T}\mathbf{Y} = \mathbf{V}\mathbf{\Sigma}^{*T}\mathbf{\Sigma}\mathbf{V}^{*T} \tag{1}$$

where V is the temporal eigenvector matrix and the diagonal values of Σ are the eigenvalue coefficients. The symbols $\left(^{*T}\right)$ indicate a conjugate transpose.

Subsequently, the eigen-components are classified using eigenvalue or eigenvector characteristics. It is assumed that the first k eigen-components form the clutter subspace [7]; hence, k is defined as the filter cutoff. Here, the cutoff is determined using two techniques: 1) identifying when the gradient of eigenvalue energy falls below a predefined level, and 2) identifying when the mean temporal eigenvector frequency exceeds a specified value. The larger eigenvalue cutoff is applied as the cutoff threshold.

This work was supported by NIBIB Grant T32-EB021937 and NSF Award IIS-1750994. Authors are with the Department of Biomedical Engineering, Vanderbilt University, Nashville, TN, 37235, USA (e-mail: kathryn.a.ozgun@vanderbilt.edu).

978-1-7281-4596-9/19/$31.00 ©2019 IEEE

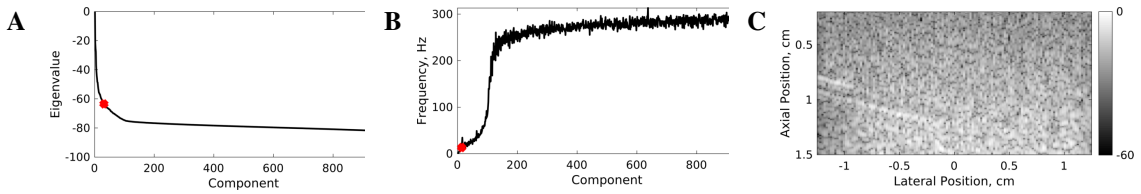

Fig. 1: The eigen-based filter cutoff was determined using (A) eigenvalue and (B) temporal eigenvector characteristics of the beamformed flow phantom data (C).

Filtering and reconstruction is accomplished by using the singular value decomposition relation,

$$\mathbf{Y} = \mathbf{U}\mathbf{\Sigma}\mathbf{V}^{*T} \tag{2}$$

From this definition, we can relate the data, $\mathbf{Y}$, to the temporal eigenvector matrix, $\mathbf{V}$, and the projection matrix, $\mathbf{X} \triangleq \mathbf{YV} = \mathbf{U}\mathbf{\Sigma}$. Thus, filtering is performed by replacing the eigencomponents containing clutter with zeros, and reconstructing the filtered dataset as follows:

$$\mathbf{V}(1:k) = 0 \tag{3}$$

$$\mathbf{X}(1:k) = 0 \tag{4}$$

$$\mathbf{Y}_{blood} = \mathbf{X}\mathbf{V}^{*T} \tag{5}$$

III. Domain-Adaptive Filtering

Delayed channel data can be represented by a four dimensional matrix, $\mathbf{Y}_{chan}$, with dimensions $(n_z \times n_x \times n_c \times n_t)$ corresponding to axial space, lateral space, channels, and time. Several adaptive beamformers operate on the channel data for each lateral beam [10], [11], so we can alternatively consider the delayed channel data to be a set of n_x submatrices, $\mathbf{Y}_{chan} = \{\mathbf{Y}_1, \mathbf{Y}_2 ... \mathbf{Y}_{n_x}\}$, each of size $(n_z \times n_c \times n_t)$.

The motivation for a domain-adaptive method is the computational complexity of generating adaptive basis sets. For a $(n_1 \times n_2)$ matrix, the calculation of a covariance matrix is associated with an $\mathcal{O}(n_1 n_2^2)$ computational burden and an eigenvalue decomposition is $\mathcal{O}(n_2^3)$. As a result, generating n_x basis sets to filter each channel submatrix is not practical.

A. Basis Generation

To reduce the computational complexity, we propose to generate the basis set using a reference RF dataset, $\mathbf{Y}_{RF}$, which is simply the sum of the delayed channel data, *i.e.*

$$\mathbf{Y}_{RF} = \sum_{j=1}^{n_c} \mathbf{Y}_{chan} \tag{6}$$

The RF dataset is reshaped into Casorati form and decomposed to obtain the basis set $\mathbf{V}$. As described in Section II, a cutoff value k can be determined from an assessment of eigencomponent characteristics.

B. Projection and Clutter Rejection

A given channel submatrix, $\mathbf{Y}_i$, where $i = [1 : n_x]$, can be projected onto the RF-defined subspace, as

$$\mathbf{X}_i = \mathbf{Y}_i\mathbf{V} \tag{7}$$

The data may be filtered by first setting the first k eigenvalues to zero, then reconstructing the filtered data matrix as

$$\mathbf{V}(1:k) = 0 \tag{8}$$

$$\mathbf{X}_i(1:k) = 0 \tag{9}$$

$$\mathbf{Y}_{i,blood} = \mathbf{X}_i\mathbf{V}^{*T} \tag{10}$$

Subsequently, the filtered channel data may be passed to an adaptive beamformer to complete image formation.

IV. Methods

A polyvinyl-alcohol (PVA) and graphite vessel phantom was constructed for validation [16]. A single vessel was formed by placing a 0.6 mm diameter wire through the mold during construction. Blood mimicking fluid (CIRS Model 046, Norfolk, VA, USA) was perfused through the vessel at 5 cm/s (90 μl/min) using a syringe pump.

Nine angled plane wave transmits spanning from -8° to 8°, spaced by 2°, were acquired using a L12-5 probe at 7.8125 MHz on a Verasonics research system (Verasonics Inc., Kirkland, WA). During acquisition, the probe was held by a volunteer sonographer to incur realistic clutter motion profiles.

One second of data was processed to form power Doppler (PD), CFPD, and ppCFPD images [10], [11]. Plane wave synthetic focusing and Hann apodization were used during beamforming, yielding a final PRF of 1000 Hz [17]. Adaptive demodulation was applied using a kernel size of 10 λ and a lag of 1 frame [18].

Clutter rejection for CFPD and ppCFPD was performed using the domain-adaptive framework of Section III. The conventional eigen-based filter presented in Section II was used for PD processing and to generate the basis model of Subsection III-A. The eigen-based filter cutoff was determined using a 20 Hz frequency cutoff and an eigenvalue threshold set to 25% of the maximum energy, as depicted in Figure 1. The eigen-based filters were compared to a 6^{th} order Chebyshev filter with a 20 Hz cutoff.

V. Results and Conclusions

Figure 2 depicts preliminary efficacy of the domain-adaptive filtering technique for adaptive beamforming. Adaptive beamformers, such as CFPD and ppCFPD, offer improved suppression of thermal noise and acoustic clutter in comparison to conventional PD. In comparison to matched PD images, CFPD and ppCFPD improved contrast up to 4.28 and 6.37 dB, respectively.

TABLE I: Image Quality Metrics for Phantom Study

	IIR Filter		Eigen-based Filter	
	Contrast, dB	**CNR**	**Contrast, dB**	**CNR**
PD	10.47	1.02	13.84	1.14
CFPD	13.42	1.03	18.12	1.14
ppCFPD	12.77	0.98	20.21	1.11

All techniques demonstrated contrast improvements when an eigen-based clutter was used, in agreement with prior literature [7]. The conventional eigen-based filter increased PD image contrast by 3.37 dB, in comparison to the IIR filter. The domain-adaptive filter increased contrast by 7.44 dB for ppCFPD and by 4.70 dB for CFPD.

We anticipate that this technique would remain effective when applied in conjunction with other eigen-based frameworks, such as blockwise [15], sparse [19], or parallel [20] implementations. Overall, research of channel domain filtering remains limited despite substantial advancements in adaptive filtering techniques. Further investigation of efficient filtering methods will likely enable greater integration of advanced beamforming and filtering techniques.

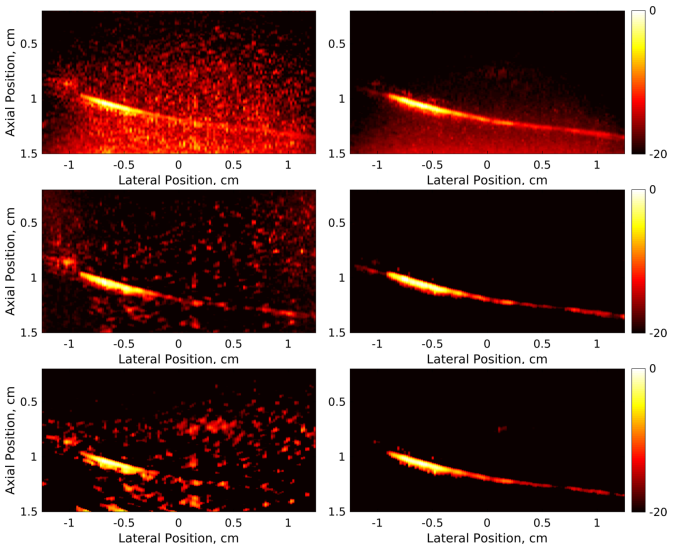

Fig. 2: Comparison of PD (top row), CFPD (middle row), ppCPFD (bottom row) images formed using highpass (left) and eigen-based (right) filtering.

Acknowledgment

The authors would like to thank the staff of the Vanderbilt University ACCRE computing resource.

References

[1] H. Torp, "Clutter rejection filters in color flow imaging: A theoretical approach," *IEEE transactions on ultrasonics, ferroelectrics, and frequency control*, vol. 44, no. 2, pp. 417–424, 1997.

[2] C. Huang, P. Song, P. Gong, J. D. Trzasko, A. Manduca, and S. Chen, "Debiasing-based noise suppression for ultrafast ultrasound microvessel imaging," *IEEE transactions on ultrasonics, ferroelectrics, and frequency control*, 2019.

[3] S. Bjaerum, H. Torp, and K. Kristoffersen, "Clutter filters adapted to tissue motion in ultrasound color flow imaging," *IEEE transactions on ultrasonics, ferroelectrics, and frequency control*, vol. 49, no. 6, pp. 693–704, 2002.

[4] F. W. Mauldin, D. Lin, and J. A. Hossack, "The singular value filter: A general filter design strategy for pca-based signal separation in medical ultrasound imaging," *IEEE transactions on medical imaging*, vol. 30, no. 11, pp. 1951–1964, 2011.

[5] J. J. Dahl and N. M. Sheth, "Reverberation clutter from subcutaneous tissue layers: Simulation and in vivo demonstrations," *Ultrasound in medicine & biology*, vol. 40, no. 4, pp. 714–726, 2014.

[6] A. Heimdal and H. Torp, "Ultrasound doppler measurements of low velocity blood flow: limitations due to clutter signals from vibrating muscles," *IEEE transactions on ultrasonics, ferroelectrics, and frequency control*, vol. 44, no. 4, pp. 873–881, 1997.

[7] A. Yu and L. Lovstakken, "Eigen-based clutter filter design for ultrasound color flow imaging: A review," *IEEE transactions on ultrasonics, ferroelectrics, and frequency control*, vol. 57, no. 5, pp. 1096–1111, 2010.

[8] C. H. Leow, N. L. Bush, A. Stanziola, M. Braga, A. Shah, J. Hernández-Gil, N. J. Long, E. O. Aboagye, J. C. Bamber, and M.-X. Tang, "3-d microvascular imaging using high frame rate ultrasound and asap without contrast agents: Development and initial in vivo evaluation on nontumor and tumor models," *IEEE transactions on ultrasonics, ferroelectrics, and frequency control*, vol. 66, no. 5, pp. 939–948, 2019.

[9] A. Stanziola, C. H. Leow, E. Bazigou, P. D. Weinberg, and M.-X. Tang, "Asap: Super-contrast vasculature imaging using coherence analysis and high frame-rate contrast enhanced ultrasound," *IEEE transactions on medical imaging*, vol. 37, no. 8, pp. 1847–1856, 2018.

[10] Y. L. Li and J. J. Dahl, "Coherent flow power doppler (cfpd): flow detection using spatial coherence beamforming," *IEEE transactions on ultrasonics, ferroelectrics, and frequency control*, vol. 62, no. 6, pp. 1022–1035, 2015.

[11] K. Ozgun, J. Tierney, and B. Byram, "An adapted coherent flow power doppler beamforming scheme for improved sensitivity towards blood signal energy," in *2018 IEEE International Ultrasonics Symposium (IUS)*. IEEE, 2018, pp. 1–4.

[12] J. J. Dahl and Y. Li, "Coherent color flow imaging: Velocity estimation using coherent signals," in *Biomedical Imaging (ISBI 2017), 2017 IEEE 14th International Symposium on*. IEEE, 2017, pp. 240–243.

[13] F. Song, D. Zhang, and X. Gong, "Performance evaluation of eigendecomposition-based adaptive clutter filter for color flow imaging," *Ultrasonics*, vol. 44, pp. e67–e71, 2006.

[14] C. Kargel, G. Hobenreich, B. Trummer, and M. F. Insana, "Adaptive clutter rejection filtering in ultrasonic strain-flow imaging," *IEEE transactions on ultrasonics, ferroelectrics, and frequency control*, vol. 50, no. 7, pp. 824–835, 2003.

[15] P. Song, A. Manduca, J. D. Trzasko, and S. Chen, "Ultrasound small vessel imaging with block-wise adaptive local clutter filtering," *IEEE transactions on medical imaging*, vol. 36, no. 1, pp. 251–262, 2017.

[16] J. Tierney, K. Walsh, H. Griffith, J. Baker, D. Brown, and B. Byram, "Combining slow flow techniques with adaptive demodulation for improved perfusion ultrasound imaging without contrast," *IEEE transactions on ultrasonics, ferroelectrics, and frequency control*, 2019.

[17] G. Montaldo, M. Tanter, J. Bercoff, N. Benech, and M. Fink, "Coherent plane-wave compounding for very high frame rate ultrasonography and transient elastography," *IEEE transactions on ultrasonics, ferroelectrics, and frequency control*, vol. 56, no. 3, pp. 489–506, 2009.

[18] J. Tierney, C. Coolbaugh, T. Towse, and B. Byram, "Adaptive clutter demodulation for non-contrast ultrasound perfusion imaging," *IEEE transactions on medical imaging*, vol. 36, no. 9, pp. 1979–1991, 2017.

[19] P. Li, X. Yang, D. Zhang, and Z. Bian, "Adaptive clutter filtering based on sparse component analysis in ultrasound color flow imaging," *IEEE transactions on ultrasonics, ferroelectrics, and frequency control*, vol. 55, no. 7, pp. 1582–1596, 2008.

[20] A. J. Chee, B. Y. Yiu, and C. Alfred, "A gpu-parallelized eigen-based clutter filter framework for ultrasound color flow imaging," *IEEE transactions on ultrasonics, ferroelectrics, and frequency control*, vol. 64, no. 1, pp. 150–163, 2016.